The final publication is available at

https://doi.org/10.1002/cepa.1777

Additional Information

Post-fire residual strength and ductility of structural steels from hollow sections

David Pons[1], Andrés Lapuebla-Ferri[1] and Manuel L. Romero[2]

Correspondence

Dr. Andrés Lapuebla-Ferri
Universitat Politècnica de València
Department of Continuum Mechanics and
Theory of Structures
Camí de Vera, s/n
46022 València, Spain
Email: anlafer0@mes.upv.es

Abstract

Steel structures are severely affected by the extreme temperatures reached during a fire. After this, if the structure has not collapsed, the remaining elements can be reused if they are not excessively distorted or the material is still fit for service. In the last case, residual properties of steel must be adequate and fulfil the requirements of the current standards. On this matter, it is hypothesized that residual behaviour of steel not only depends on the highest temperature reached during the fire episode, but also on the load it was simultaneously bearing.

This work is focused on an experimental study on the post-fire behaviour of structural steels. Specimens were cut from structural steel (S355) cold-formed circular hollow sections (CHS) and subjected to a combination of tensile stress and high temperature. Afterwards, the specimens were cooled in air back to room temperature and, finally, load was increased until specimen failure. The obtained results allowed discussing on the residual yield strength, ultimate strength and stiffness of the steel, and a special focus was put on the residual ductility. The results of this work can provide a basis to the appraisal of steel structures after fire, supporting the further decision on its reinstatement or subsequent demolition.

Keywords

Post-fire behaviour, Structural steel, Residual properties, Yield strength, Ultimate strength, Stiffness, Ductility, Hollow sections.

1 Introduction

Steel is a very spread construction material used in framed structures for industrial, residential, commercial or government buildings. According to its mechanical properties, the advantages of using steel are well known and beyond doubt.

However, structural steel has a high thermal conductivity, so the high temperatures reached during a fire episode reduce considerably its mechanical performance. If the structure survives to the fire, it must be evaluated if it can still be put again into service – and the associated costs – or it has to be demolished instead.

Since years, this topic has attracted the attention of structural engineers [1-2]. A criterion traditionally followed during post-fire inspection is that the structure is still able to service if the elements are not severely distorted [3]. This statement is also found in the form of advice in British Standard 5950 [4], one of the few codes that refer to the post-fire situation of a steel structure.

1. Dpt. of Continuum Mechanics and Theory of Structures. Universitat Politècnica de València, Spain.

2. ICITECH. Universitat Politècnica de València, Spain.

However, the deformation of the structure not always can be related to the temperature attained during fire [5] and the residual properties of the steel depend on the maximum temperature it was heated to. In order to decide on the reinstatement or demolition of the surviving structure, the post-fire properties of the steel must be obtained and compared with the provisions of the current standards, so experimental testing is a reliable option.

This topic has been studied in previous experimental works on cold-formed steels [6-7], structural steels [8-10], high-strength steels [11-12] and stainless structural steels [13]. In these works, however, the tested specimens were subjected to a heating and cooling thermal cycle while remained unloaded. This is not a realistic situation, since during a fire event a structural element is bearing, at least, its own weight. Thus, the stress level that the steel was bearing at the onset on fire is expected to influence on its post-fire behaviour.

This paper focuses on an experimental investigation of the residual mechanical properties of structural steel after fire. Specimens were extracted from cold-formed CHS and were subjected to a combination of tensile stress and high temperature (from room

temperature to 1000 °C). Then, specimens were left to cool down to room temperature and submitted to tensile testing. The influence of tensile stress along with a heating and cooling cycle in the post-fire mechanical behaviour of structural steel was evaluated (residual values of yield strength, ultimate strength and stiffness). A special attention was put on residual ductility, which is quantified and compared with the provisions of Eurocode 3 [14]. A similar approach was carried out in a recent work of Lapuebla-Ferri et al. [15], but applied to steel reinforcing bars for reinforced concrete structures.

2   Materials and methods

2.1   Overview

The specimens under study (sub-section 2.2) were firstly subjected to tensile testing in order to obtain its main mechanical features at room temperature (sub-section 2.3).

Posteriorly, in order to subject specimens to heating and cooling cycles, they were placed in an experimental setup that is described in sub-section 2.4. Three different tests at high temperatures were performed. One set of specimens was tested under a constant tensile load and an increasing temperature in order to determine the value of the 'critical temperature' θ_{crit} at which the specimen fails. These tests are known as 'transient-state tests' (section 3).

A second and third set of specimens were tested with the purpose to obtain the residual properties of steel after a fire ('post-fire tests', described in section 4). Specimens were heated to a target temperature θ_t and cooled back down to room temperature. After this, the specimen was subjected to tensile loading until failure. During the thermal cycle, one of the sets remained unloaded ('post-fire, unloaded tests', described in sub-section 4.2), while the last set was simultaneously subjected to a tensile load that remained constant throughout the test ('post-fire, loaded tests' sub-section 4.3). In every test at high temperature, a single specimen was tested.

2.2   Test specimens

Specimens were cut from CHS manufactured with steel grade S355 sheets as base material.

These tubular sections were manufactured by subjecting a steel sheet to a cold-forming process to obtain the desired cylindrical shape. Afterwards, the deformed sheet was welded along the tube length. Due to this cold-forming manufacturing process, the profiles are expected to accumulate some amount of residual stresses.

CHS were longitudinally cut in a workshop. The coupon-shaped specimens had a length of 800 mm, an average width of 23 mm and a thickness of 6 mm. In order to dispose of a set of specimens with a homogeneous material, the specimens from each tube near the welded seam were discarded.

Figure 1 Some test specimens, cut from CHS.

In Figure 1, it can be seen that the specimens acquired a curved shape, due to the presence of the aforementioned residual stresses. Notwithstanding these stresses, they were considered to not affect the results of this work.

2.3   Material properties at room temperature

A set of 4 specimens was subjected to tensile testing in order to obtain the stress-strain curves of the specimens at room temperature. From these curves, the mechanical properties of the material were extracted. The averaged mechanical features of the steel specimens cut from the tubes can be found in Table 1. It has to be into account that yield strength was measured by computing the 0.2% proof stress, because the yielding plateau of the stress-strain curves, which serves to identify the yield strength point, was not clearly visible in some tests.

Table 1 Averaged mechanical features of S355 steel from CHS sections at room temperature.

Parameter	Value
Yield strength f_y	446.84 MPa
Ultimate strength f_u	484.86 MPa
Modulus of elasticity E	208520 MPa
Ultimate strain ε_u (at f_u)	6.73 %
Strain at fracture ε_f	9.21 %

2.4   Experimental setup

The experimental setup is depicted in Figure 2. It consisted of a hydraulic universal testing machine equipped with a 200 kN calibrated load cell and controlled by a closed-loop system. The machine was equipped with hydraulic flat jaws located in the upper and lower blocks, so the tested specimen could be laterally clamped to avoid its slip. The upper block remained fixed during each test, and the lower block could move downwards in order to subject the specimen to a tensile test or to adjust its length while being heated in order to maintain a constant stress.

Besides, an electric furnace was attached to the frame of the testing machine, so the specimens could be heated. The furnace had 3 independently controlled heating zones, each one covering 1/3 of the heating chamber. Figure 2 shows that upper and lower furnace endings were insulated with rock wool to avoid heating loses, thus ensuring a uniform temperature distribution along the specimen.

The extensometer shown in Figure 2 was used to measure the modulus of elasticity of the specimen when subjected to tensile testing (gauge length 515 mm). It was attached to the central portion of the specimen, and it was removed from the setup once the plastic range was reached to avoid its breakage.

K-type thermocouples located in the middle of each heating zone measured the temperatures of the specimen surface. Thermocouples were connected to a control unit, which served to maintain an even heating of the specimen, ensuring that the desired target temperature θ_t was reached. The machine measurements, the extensometer data and the readings from the three thermocouples were recorded by using a digital acquisition system. A software installed in a computer allowed data registration and posterior analysis.
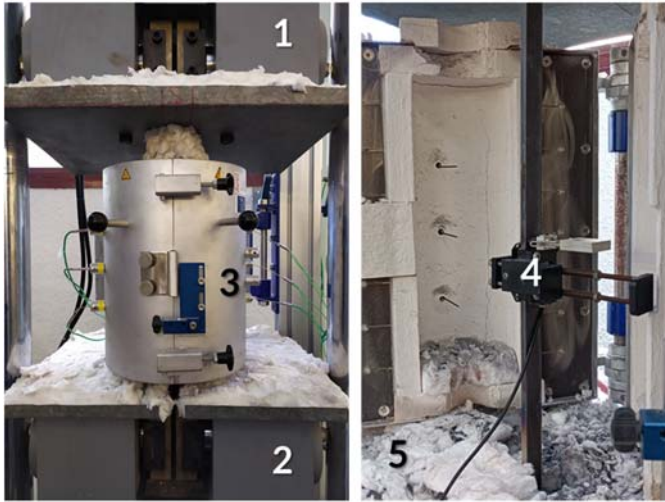
Figure 2 Experimental setup. 1) Upper block. 2) Lower block. 3) Electric furnace. 4) Extensometer. 5) Rock wool.

3   Transient-state tests

3.1   Description

'Transient-state tests' replicate a realistic situation of a structural material during fire, considering that the elements are loaded while temperature increases.

In this study, transient-state tests were used to measure the 'critical temperature' θ_{crit} of a specimen that is simultaneously subjected to a combination of tensile stress and increasing temperature. Figure 3 illustrates the time-dependent temperature and stress histories.
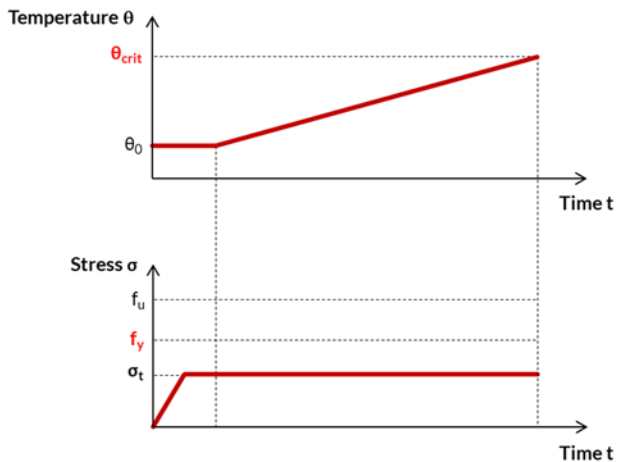

Figure 3 Transient-state tests. Temperature-time and stress-time histories.

Every specimen submitted to transient-state test was placed in the testing machine and preloaded to a tensile stress σ_t corresponding to a fraction of the yield strength f_y of the material at room temperature (see Table 1). In standards, such as Eurocode 3, part 1-2 (EN 1993-1-2 [16]), the amount of stress an element is bearing during a fire event can be computed through the parameter known as 'degree of utilisation' $\mu_0 \in (0, 1)$:

$$\mu_0 = \frac{E_{fi,d}}{R_{fi,d,0}} \qquad (1)$$

where $E_{fi,d}$ is the design effect of actions in the fire situation and $R_{fi,d,0}$ is the design value of a resistance in the fire situation at time t =0, this is, at the onset of fire.

The preload was kept constant while the specimen was heated at a constant rate of 10 °C/min until its failure. This heating rate is used in similar works found in the literature [8]. It corresponds to the heating rate during natural fire of a partially protected element (for example, by non-structural elements).

3.2   Results

In transient-state tests, the variation of strain with the temperature was recorded (Figure 4). These curves served to obtain the critical temperature θ_{crit} at which the specimen breaks for a given degree of utilisation μ_0. In the test performed at $\mu_0 = 0.5$, a failure of the registration data system avoided the temperature-strain curves to be recorded.

In each of the curves of Figure 4, the critical temperature corresponds to a 'runaway value' from which the strains of the specimen rise sharply. More precisely, it was assumed that the critical temperature θ_{crit} was attained by the specimen when the strain rate reached its maximum value of all the heating history, known as 'critical strain rate' $(\Delta\varepsilon/\Delta t)_{crit}$.
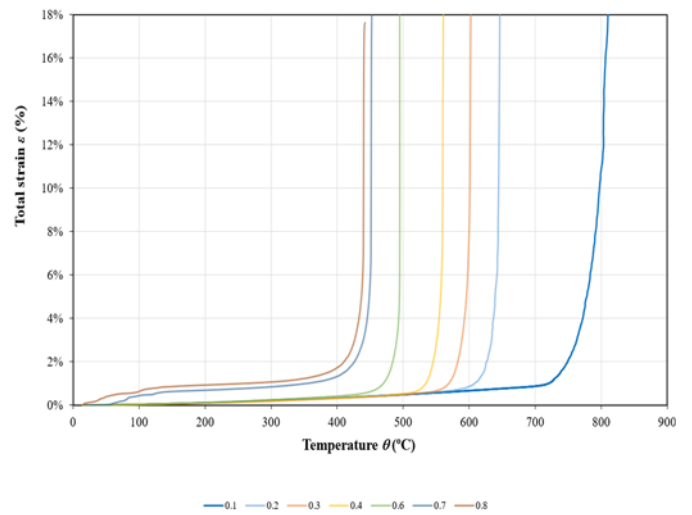

Figure 4 Transient-state tests. Strain-temperature curves for each degree of utilisation μ_0.

The critical temperature dependence on a degree of utilisation ranging from 0.1 to 0.8 is shown in Table 2. Obviously, the higher the tensile stress the specimen is subjected to, the lower is the critical temperature. It was also performed a test with a degree of utilisation $\mu_0 = 0.9$, but the associated critical temperature could not be recorded because the elongation of the specimen exceeded the stroke of the testing machine without breaking.

Table 2 Transient-state tests. Critical temperature dependence on the degree of utilisation.

μ_0	θ_{crit} (°C)	$(\Delta\varepsilon/\Delta t)_{crit}$ (s^{-1})
0.1	810.64	0.00223
0.2	645.90	0.01771
0.3	601.96	0.02243
0.4	560.23	0.02846
0.5	553.00	0.03232
0.6	494.89	0.03927
0.7	451.55	0.03549
0.8	440.16	0.03461

The variation of the critical temperature with the degree of utilisation is represented in Figure 5.
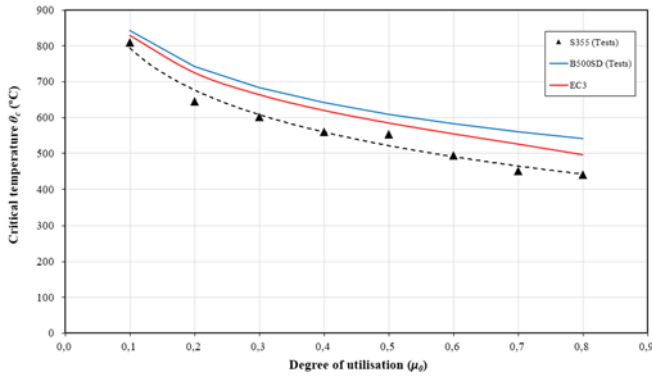
Figure 5 Transient-state tests. Critical temperature of S355 structural steel and B 500 SD reinforcing steel as a function of the degree of utilisation.

Experimental results were fitted to the logarithmic expression (2) (dashed line in Figure 5, $R^2 = 0.976$):

$$\theta_{crit} = -169.20 \cdot \ln(\mu_0) + 404.47 \qquad (2)$$

The results from another experimental works are also plotted in Figure 5 for comparison purposes. In a previous work of Lapuebla-Ferri et al [15] it was obtained the dependence of θ_{crit} on the degree of utilisation for B 500 SD reinforcing steel bars:

$$\theta_{crit} = -145.20 \cdot \ln(\mu_0) + 508.80 \qquad (3)$$

Curves from expressions (2) and (3) were compared with the following expression given in Eurocode 3, part 1-2 [16] for carbon structural steels:

$$\theta_{crit} = 39,19 \cdot \ln\left(\frac{1}{0,9674 \cdot \mu_0^{3,833}} - 1\right) + 482 \qquad (4)$$

In Figure 5, it can be shown that the experimental curves plotted from expressions (2) and (3) follow the same trend than the curve obtained by plotting expression (4). Nevertheless, the curve from (2) is below the curve from Eurocode 3, part 1-2. This means that, in specimens from cold-formed CHS tubes, the use of expression (4) to compute θ_{crit} for a given μ_0 can lead to unconservative results. The opposite can be observed if expressions (3) and (4) are compared.

4 Post-fire tests

4.1 Description

'Post-fire tests' allow to attain residual material properties for a given combination of tensile loading and a heating and cooling cycle. Figure 6 depicts the temperature-time and stress-time histories in post-fire tests.

A specimen subjected to post-fire test was placed in the testing machine and clamped at both end and it was subjected to a tensile load at room temperature θ_0 until the specimen reached a stress level σ_t (corresponding to a given degree of utilisation μ_0). The same degrees of utilisation as the transient-state tests were considered. While keeping constant σ_t, the specimen was heated until a target temperature $\theta_t < \theta_{crit}$. A heating rate of 10 °C/min, the same as the applied in transient-state tests, was also chosen.

When the furnace reached the target temperature, it was maintained during a holding time t_s of 30 min to ensure that the specimen was evenly heated. After this, the furnace was turned down and opened, allowing the specimen to gradually cool down in air back to room temperature θ_0 ('natural cooling'). During all the

cooling period, the applied tensile stress σ_t remained constant and, once room temperature was reached, the tensile load was increased until the failure of the specimen occurred at a f_u stress.
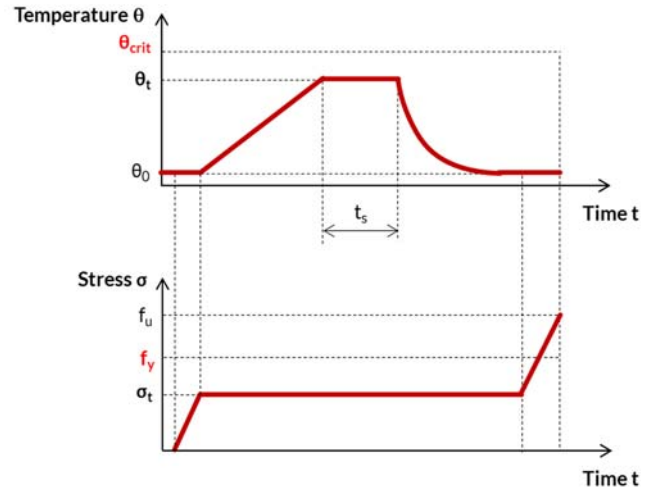

Figure 6 Post-fire tests. Temperature-time and stress-time histories.

Two different modalities of post-fire tests were performed: post-fire, unloaded tests (PFU) and post-fire, loaded tests (PFL), which are described in the following subsections.

4.2 Post-fire, unloaded tests (PFU).

PFU tests are the post-fire tests traditionally carried out in the literature, as it can be found in previous works [6-13]. In PFU tests, no load is applied, so $\sigma_t = 0$ and $\mu_0 = 0$. PFU tests were carried out for target temperatures θ_t ranging from 100 °C to 1000 °C at intervals of 100 °C.

4.2.1 Visual inspection

Figure 7 shows the failure shapes of specimens subjected to PFU tests. The different colourings of the specimens were caused by oxide formation in the outer surface of the steel specimen at θ_t. In post-fire inspection of steel structures affected by fire, surface colours can be regarded as indicators of the maximum temperature attained. Another indicator of the fire severity is related to the presence of scaling (burnt steel) when heated to 700 °C or more. Severe scaling can lead to a significant loss of cross-section.

Another indicator concerning ductility is the variation of the specimen geometry. The most evident is the elongation, which is clearly visible at 900 °C and 1000 °C. When subjeted to tensile testing, the specimen heated to 1000 °C highly increased its length up to the stroke of the testing machine without breaking.

Figure 7 Failure shapes of specimens subjected to PFU tests. In the image, the upper specimen was heated to 100 °C, and, from up to down, to increasing temperatures at intervals of 100 °C (the lower was heated to 1000 °C).

4.2.2 Residual stress-strain curves

Following PFU tests, the residual stress-strain curves could be plotted (Figure 8). The residual values of yield strength f_y (0.2% proof stress) and ultimate strength f_u are shown in Table 3, and the residual values of stiffness (elastic modulus E) and residual ductility (strain at fracture ε_f) are shown in Table 4.
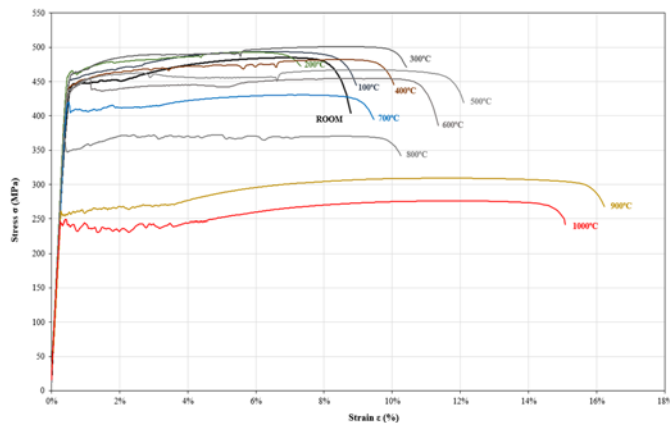

Figure 8 PFU tests. Residual stress-strain curves for unloaded specimens heated at target temperatures ranging from 100 °C to 1000 °C and cooled back to room temperature. The curve at room temperature is also plotted for comparison purposes.

Table 3 PFU tests. Residual values and residual factors (R. F.) of yield strength f_y and ultimate strength f_u.

θ_t (°C)	f_y (MPa)	R. F.	f_u (MPa)	R. F.
20	**446.84**	**1.00**	**484.86**	**1.00**
100	452.42	1.01	493.79	1.02
200	462.54	1.04	492.80	1.02
300	459.77	1.03	500.91	1.03
400	445.40	1.00	482.10	0.99
500	441.03	0.99	467.03	0.96
600	441.06	0.99	454.79	0.94
700	407.32	0.91	430.58	0.89
800	349.03	0.78	372.32	0.77
900	255.73	0.57	309.28	0.64
1000	246.23	0.55	276.01	0.57

Table 4 PFU tests. Residual values and residual factors (R. F.) of stiffness (modulus of elasticity E) and ductility (strain at fracture ε_f).

θ_t (°C)	E (MPa)	R. F.	ε_f (%)	R. F.
20	**208520**	**1.00**	**9.21**	**1.00**
100	206522	0.99	9.55	1.04
200	201596	0.97	8.17	0.89
300	200000	0.96	11.12	1.21
400	207108	0.99	10.67	1.16
500	207000	0.99	12.74	1.38
600	203000	0.97	11.84	1.29
700	184000	0.88	10.13	1.10
800	208900	1.00	10.92	1.19
900	180000	0.86	16.80	1.82
1000	193117	0.93	15.09	1.64

When heated up to 300 °C, residual values of yield strength, ultimate strength and ductility increase with respect to the values measured at room temperature. At 400 °C, the values of these properties at room temperature are almost completely retained. Within the range 500 °C-700 °C, residual yield strength and ultimate strength start to decrease slightly, showing a recovery close to 90% of the values at room temperature after cooling down from 700 °C. However, when heated to 800 °C or higher temperatures and cooled down, residual yield and ultimate strengths decrease drastically. At 1000 °C, these values have been reduced to less than 60% of the measured at room temperature.

With regard to the residual stiffness of steel, it can be observed that the value of the elasticity modulus (this is, the slope of the linear portion of the stress-strain curves) is practically the same for all the studied temperature range. Stiffness remained almost completely unaffected when heated to any target temperature of the studied range and posteriorly cooled down to room temperature. This behaviour was also observed in the previous works [8] [15].

As it is shown in Figure 8, residual ductility increases with θ_t. Changes in ductility can be appreciated in the extension of the plastic portion of the residual stress-strain curves and a pronounced yielding plateau, as well as in the broken specimens of Figure 7. Exceptionally, ductility decreases after cooling down from 700 °C, a value near the eutectoid temperature of steel. The crystallographic transformations that occur in the material can explain this phenomenon, as well as the residual ductility almost doubles for 900 °C. At 1000 °C, the residual value of the strain at fracture is a 64% higher than the measured at room temperature.

4.2.3 Residual factors

The 'residual factor' of a mechanical property is the ratio between the value of that property measured in PFU test to the value at room temperature. The residual factors are found in Table 3 and Table 4. A residual factor quantifies how amount of a given property is retained after cooling down. Graphs of Figure 9 (a-c) illustrate the variation of residual factors of f_y, f_u and E with the target temperature, as they were measured in PFU tests.
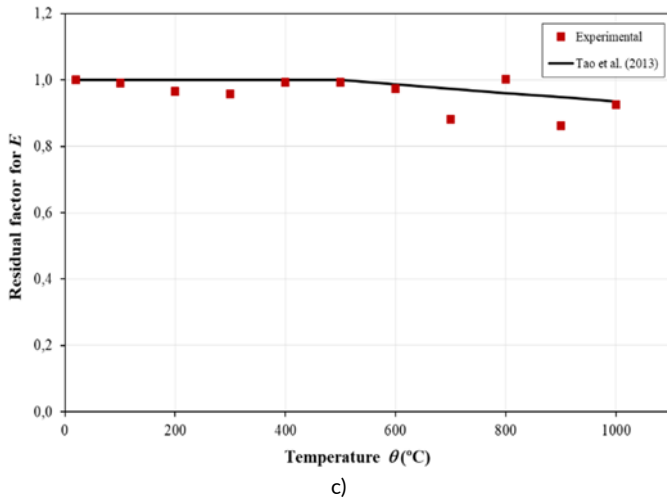

a)

b)
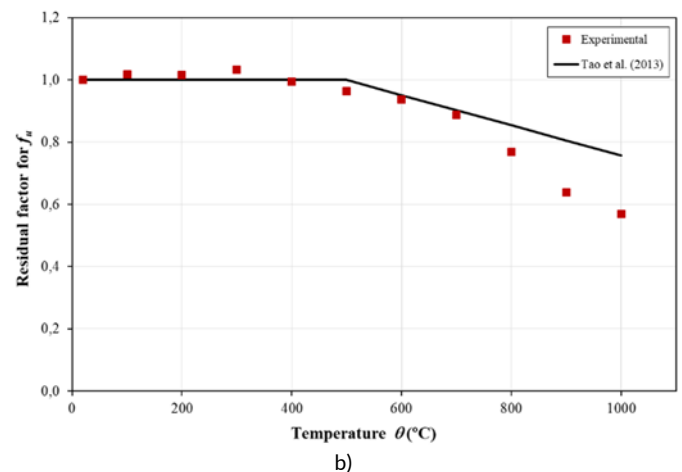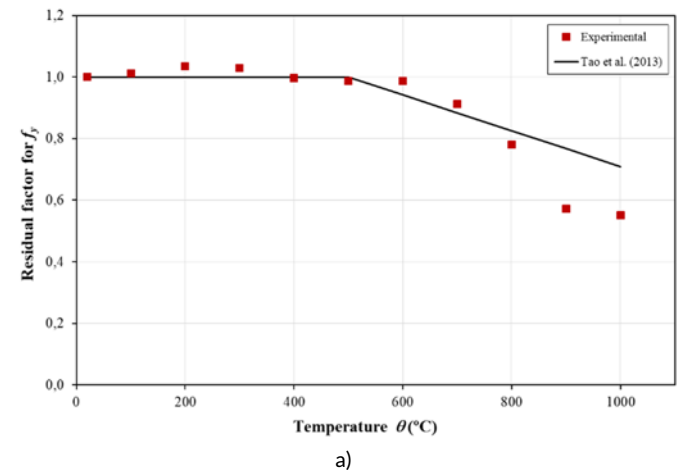
Figure 9 PFU tests (PFU). Retention factors for: a) yield strength f_y, b) ultimate strength f_u and c) elastic modulus E.

In these graphs, the trends obtained in a previous work from Tao et al. [9] are also represented. It can be observed a good agreement between the results obtained in this work and those obtained in the aforementioned study.

4.3 Post-fire. loaded tests (PFL)

To the best of the authors' knowledge, the joint influence of high temperature and load in the post-fire behaviour of structural materials has been studied in only a few works (see [15]).

Unlike PFU tests, specimens in PFL tests were preloaded to a tensile stress $\sigma_t \neq 0$, thus the degree of utilisation was $\mu_0 > 0$. This stress was kept constant during heating of the specimen at a constant rate up to a target temperature $\theta_t < \theta_{crit}$. Once the specimen was evenly heated, it was left to cool down in air back to room temperature. Finally, the tensile stress was increased, submitting the specimen to tensile testing up to its failure.

Table 5 summarizes the PFL tests carried out. The first two rows show, respectively, the degree of utilisation μ_0 and the corresponding critical temperature θ_{crit} measured in transient-state tests. The same range of target temperatures in PFL tests was chosen to be the same than PFU (from 100 °C to 1000 °C at 100 °C intervals) in order to compare results.

In Table 5, the intersection of the row for a given target temperature θ_t with the column for a certain degree of utilisation μ_0 provides a percentage, which is the amount of the critical temperature θ_{crit} that is the target temperature θ_t for that degree of utilisation μ_0. For example, considering a specimen with a degree of utilisation $\mu_0 = 0.4$ heated up to 400 °C, this target temperature is a 71% of the corresponding θ_{cri}.

Among all the combinations given in Table 5, only the PFL tests at target temperatures from 400 °C to 700 °C were performed for a limited number of degrees of utilisation. The reason is twofold. Firstly, a test could not be obviously performed if, for a given value of μ_0, $\theta_t > \theta_{crit}$. These situations are the blank cells of Table 5. Secondly, PFU tests revealed that target temperatures $\theta_t \leq 300$ °C had little or no influence on the post-fire behaviour of steel. This behaviour was assumed to repeat even for loaded specimens.

Considering all these aspects, there were performed only the tests with the combinations of θ_t and μ_0 falling into the shaded cells of Table 5. Tests at $\theta_t = 400$ °C and degrees of utilisation μ_0 equal to 0.3,

0.5 and 0.7 were not be carried out for time-saving purposes (empty cells in the row of 400 °C).

Table 5 PFL Tests. Different combinations of degrees of utilisation and target temperatures.

μ_0	0.1	0.2	0.3	0.4	0.5	0.6	0.7	0.8
θ_{crit} (°C)	810	648	602	560	553	495	455	440
θ_t (°C)				% θ_{crit} (°C)				
100	12%	15%	17%	18%	18%	20%	22%	23%
200	25%	31%	33%	36%	36%	40%	44%	45%
300	37%	46%	50%	54%	54%	61%	66%	68%
400	49%	62%		71%		81%		**91%**
500	62%	77%	83%	89%	90%			
600	74%	93%						
700	86%							
800								
900								
1000								

4.3.1 Visual inspection

Figure 10 shows the failure shapes of specimens from PFL tests.

If failure shapes of Figure 7 and Figure 10 are compared, there can be observed several differences. In PFL tests, the failure shapes acquired a more rounded shape than the observed for PFU tests. Differences in necking can be appreciated, too. Quantitative measures will explain if these changes are related to differences in the residual ductility behaviour of PFU and PFL tests, but this is not an objective of the present work.

Figure 10 Specimens subjected to PFL tests. Failure shapes.

4.3.2 Residual stress-strain curves and residual factors

From each PFL test carried out, a residual stress-strain curve was plotted. Figure 11 and Figure 12 show the stress-strain curves obtained for target temperatures θ_t equal to 400 °C and 500 °C, respectively, and different degrees of utilisation μ_0. Stress-strain curves at room temperature and the obtained in a PFU test for that θ_t are also plotted. In Figure 11, PFL test subjected to $\mu_0 = 0.8$ and heated to $\theta_t = 400$ °C (91% of θ_{crit}) could not be finished because the specimen broke during holding time, probably due to creep effects due to the combination of tensile loading and temperature.

The values of yield strength f_y, ultimate strength f_u, elastic modulus E and strain at failure ε_f were recorded for 400 °C and 500 °C and different degrees of utilisation. These values, as well as the pertinent residual factors are shown respectively in Table 6 and Table 7. In

these tables, 'N/R' means that some values could not be registered due to measurement errors.
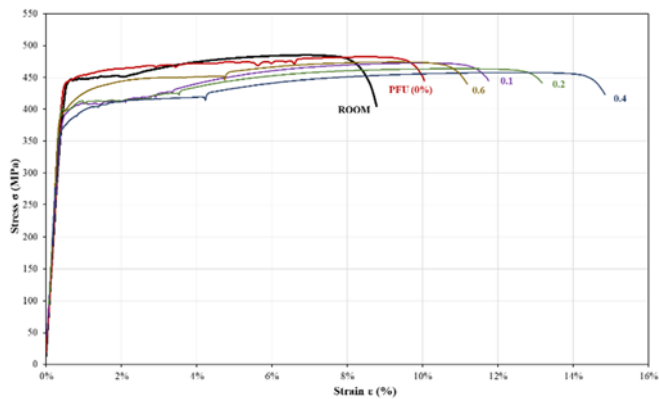

Figure 11 PFL tests. Residual stress-strain curves for specimens with different degrees of utilisation heated to 400 °C and cooled down to room temperature.
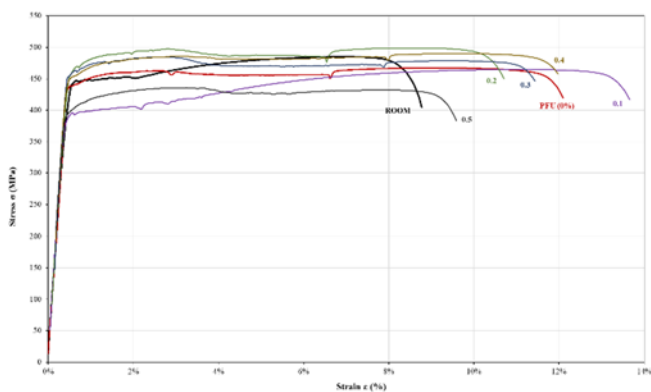

Figure 12 PFL tests. Residual stress-strain curves for specimens with different degrees of utilisation heated to 500 °C and cooled down to room temperature.

Table 6 PFL tests at 400°C. Residual values and residual factors (R. F.) of yield strength f_y, ultimate strength f_u, stiffness (modulus of elasticity E) and ductility (strain at fracture ε_f).

μ_0	f_y (MPa)	R. F.	f_u (MPa)	R. F.	E (MPa)	R. F.	ε_f (%)	R. F.
0	445.40	1.00	482.10	0.99	207108	0.99	10.67	1.16
0.1	381.00	0.85	472.58	0.97	N/R	N/R	12.51	1.36
0.2	380.95	0.85	463.48	0.96	194602	0.93	13.96	1.52
0.4	383.95	0.86	457.50	0.94	189472	0.91	15.49	1.68
0.6	383.25	0.86	474.17	0.98	185916	0.89	11.90	1.29

Table 7 PFL tests at 500°C. Residual values and residual factors (R. F.) of yield strength f_y, ultimate strength f_u, stiffness (modulus of elasticity E) and ductility (strain at fracture ε_f).

μ_0	f_y (MPa)	R. F.	f_u (MPa)	R. F.	E (MPa)	R. F.	ε_f (%)	R. F.
0	441.03	0.99	467.03	0.96	207000	0.99	12.74	1.38
0.1	376.44	0.84	464.70	0.96	227890	1.09	14.26	1.55
0.2	448.62	1.00	498.86	1.03	219252	1.05	11.36	1.23
0.3	442.72	0.99	484.62	1.00	N/R	N/R	12.18	1.32
0.4	434.26	0.97	489.85	1.01	178145	0.85	12.76	1.39
0.5	418.69	0.94	435.63	0.90	184436	0.88	10.16	1.10

From these values, it can be deducted that heating up to 400 °C for the given degrees of utilisation decreases the yield strength to an 85% of its value at room temperature, while this value was kept for the same target temperature in the PFU test. This is less evident for a heating to 500 °C since f_y seems to be kept (excepting for $\mu_0 = 0.1$). Regarding ultimate stress f_u, the value at room temperature seems to be maintained when specimen is subjected to simultaneous tensile loading and heating up to 400 °C and 500 °C.

Modulus of elasticity E shows a decreasing trend with the degree of utilisation μ_0. For 400 °C ($\mu_0 = 0.6$) and 500 °C ($\mu_0 = 0.5$) the residual value is similar to the measured for PFU tests at a target temperature of 700 °C, so differences in material stiffness between PFU and PFL tests are appreciated.

Regarding residual ductility, for a target temperature of 400 °C it increases with the degree of utilisation up to $\mu_0 = 0.4$. At $\mu_0 = 0.6$, this trend seems to reverse. Nevertheless, in the studied range of μ_0, the residual ductility is higher than the measured from PFU tests. For 500 °C this is less evident, since for $\mu_0 = 0.1$ to $\mu_0 = 0.4$ ductility seems to oscillate around the value measured in PFU tests. On the contrary, for $\mu_0 = 0.5$ ductility is lower than the measured in PFU test.

In a complementary manner, Figure 13 shows the residual stress-strain curves corresponding to specimens subjected to a degree of utilisation $\mu_0 = 0.1$ and heated to different target temperatures ranging from 400 °C to 700 °C. As it can be appreciated, the material properties are reduced with respect of the measured at room temperature. On the other hand, residual ductility increases up to 600 °C and decreases abruptly at 700 °C. In spite of this, it can be observed than the ductility is higher than the measured at room temperature in the full range of the studied temperatures.
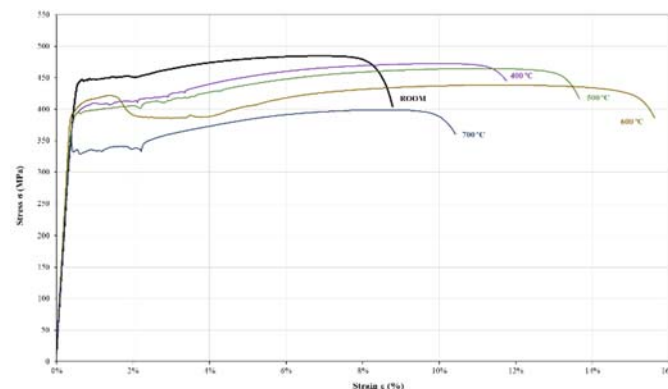

Figure 13 PFL tests. Residual stress-strain curves for specimens heated to temperatures ranging from 400 °C to 700 °C and loaded to a degree of utilisation $\mu_0 = 0.1$.

5   Post-fire residual ductility and code provisions

'Ductility' is the ability of a structural material to withstand deformations without breaking. This is a paramount aspect to consider in steel structures located in high-risk seismic areas.

In this section, it is intended to evaluate the influence of applied load along with heating and cooling in the post-fire ductility behaviour of steel, so results from PFU and PFL tests are compared with the provisions from Eurocode 3, part 1-1 [14]. According to it, structural steels are required to have a minimum ductility, which should be expressed in the following conditions:

1. Ratio ultimate strength to yield strength $f_u/f_y \geq 1.1$.
2. Strain at fracture $\varepsilon_f \geq 15\%$.
3. Ratio ultimate strain to yield strain $\varepsilon_u / \varepsilon_y \geq 15$, where ε_y is the strain at yield strength.

Such conditions must be simultaneously satisfied. The numerical values of the limits are recommendations given in the Eurocode 3.

In Table 8, the results of PFU tests can be found in order to evaluate the fulfilment of the first two conditions. The ratio f_u/f_y is verified for all the heating range but, surprisingly, condition $\varepsilon_f \geq 15\%$ is not verified for almost all the temperature range, even at room temperature, except for 900 °C and 1000 °C. This may be justified because the specimens come from cold-formed CHS sections, whilst the ductility conditions found in the Eurocode 3 are intended to be used in hot-rolled structural steels. In spite of this, it is seen that the strain at failure ε_f follows an increasing trend along the studied range of temperatures.

Table 8 PFU Tests. Ductility indicators from Eurocode 3 f_u/f_y and ε_f.

θ_t (°C)	f_y (MPa)	f_u (MPa)	f_u/f_y	ε_f (%)
20	**446.84**	**484.86**	**1.1**	**9.21**
100	452.42	493.79	1.1	**9.55**
200	462.54	492.80	1.1	**8.17**
300	459.77	500.91	1.1	**11.12**
400	445.40	482.10	1.1	**10.67**
500	441.03	467.03	1.1	**12.74**
600	441.06	454.79	1.0	**11.84**
700	407.32	430.58	1.1	**10.13**
800	349.03	372.32	1.1	**10.92**
900	255.73	309.28	1.2	16.80
1000	246.23	276.01	1.1	15.09

Table 9 shows the verification of the ductility requirement $\varepsilon_u / \varepsilon_y \geq 15$. These values indicate that the only target temperature that does not fulfil the minimum value is 800 °C. This result can be explained by the proximity of this target temperature to the eutectoid temperature of steel.

Table 9 PFU Tests. Ductility indicator from Eurocode 3 $\varepsilon_u/\varepsilon_y$.

θ_t (°C)	f_y (MPa)	E (MPa)	ε_y (%)	ε_u (%)	$\varepsilon_u / \varepsilon_y$
20	**446.84**	**208520**	**0.21**	**6.73**	**31.41**
100	452.42	206522	0.22	6.35	28.99
200	462.54	201596	0.23	5.71	24.89
300	459.77	200000	0.23	8.24	35.84
400	445.40	207108	0.22	8.36	38.87
500	441.03	207000	0.21	8.80	41.30
600	441.06	203000	0.22	9.33	42.94
700	407.32	184000	0.22	7.39	33.38
800	349.03	208900	0.17	2.41	**14.42**
900	255.73	180000	0.14	11.64	81.93
1000	246.23	193117	0.13	11.64	91.29

Table 10 and Table 11 show the verification of the first and second ductility requirements for PFL tests (target temperatures of 400 °C and 500 °C, respectively).

Table 10 PFL Tests. Target temperature of 400 °C. Ductility indicators from Eurocode 3 f_u/f_y and ε_f.

μ_0	f_y (MPa)	f_u (MPa)	f_u/f_y	ε_f (%)
0	**445.40**	**482.10**	**1.1**	**10.67**
0.1	381.00	472.58	1.2	**12.51**
0.2	380.95	463.48	1.2	**13.96**
0.4	383.95	457.50	1.2	**15.49**
0.6	383.25	474.17	1.2	**11.90**

Table 11 PFL Tests. Target temperature of 500 °C. Ductility indicators from Eurocode 3 f_u/f_y and ε_f.

μ_0	f_y (MPa)	f_u (MPa)	f_u/f_y	ε_f (%)
0	**441.03**	**467.03**	**1.1**	**12.74**
0.1	376.44	464.70	1.2	**14.26**
0.2	448.62	498.86	1.1	**11.36**
0.3	442.72	484.62	1.1	**12.18**
0.4	434.26	489.85	1.1	**12.76**
0.5	418.69	435.63	**1.0**	**10.16**

In Table 10 and Table 11, the ratio f_u/f_y is verified for the entire range of degrees of utilisation, excepting for $\mu_0 = 0.5$ and 500 °C. Again, the requirement $\varepsilon_f \geq 15\%$ is not verified for the reasons given before.

Tables 12 and 13 show the verification of the ductility requirement $\varepsilon_u / \varepsilon_y \geq 15$ in PFL tests with target temperatures of 400 °C and 500 °C. It can be seen that the only PFL test in which code requirements for residual ductility are not verified is the test performed for a target temperature of 500 °C.

In addition, from the point of view of the ductility indicator $\varepsilon_u / \varepsilon_y$, it is observed a pronounced reduction of residual ductility when PFL test results performed at $\mu_0 > 0$ are compared to the result from the test performed at $\mu_0 = 0$.

Table 12 PFL Tests. Target temperature of 400 °C. Ductility indicator from Eurocode 3 $\varepsilon_u/\varepsilon_y$.

μ_0	f_y (MPa)	E (MPa)	ε_y (%)	ε_u (%)	$\varepsilon_u / \varepsilon_y$
0	**445.40**	**207108**	**0.22**	**8.36**	**38.87**
0.1	381.00	N/R	N/R	9.85	N/R
0.2	380.95	194602	0.20	10.53	53.79
0.4	383.95	189472	0.20	12.47	61.54
0.6	383.25	185916	0.21	9.09	44.10

Table 13 PFL Tests. Target temperature of 500 °C. Ductility indicator from Eurocode 3 $\varepsilon_u/\varepsilon_y$.

μ_0	f_y (MPa)	E (MPa)	ε_y (%)	ε_u (%)	$\varepsilon_u / \varepsilon_y$
0	**441.03**	**207000**	**0.21%**	**8.80%**	**41.30**
0.1	376.44	227890	N/R	10.98%	N/R
0.2	376.44	219252	0.17%	8.33%	48.52
0.3	448.62	N/R	N/R	8.45%	N/R
0.4	442.72	178145	0.25%	9.36%	37.66
0.5	434.26	184436	0.24%	3.25%	**13.80**

6 Conclusions

In the present work, an experimental campaign was carried out in order to evaluate the residual mechanical properties of coupon-shaped specimens cut from cold-formed CHS of structural steel S355 after its exposition to a combination of tensile loading and high temperature.

This is a realistic situation, because when a fire ignites in a building the structure its bearing certain amount of load, represented by the 'degree of utilisation' parameter μ_0 as it is defined in Eurocode 3, part 1-2.

Specimens were subjected to a certain degree of utilisation μ_0 and heated until a target temperature $\theta_t < \theta_{crit}$ was reached. θ_{crit} was the temperature at which a specimen broke when it was subjected to

simultaneous uniform heating and tensile stress, and it was obtained by transient-state tests. Posteriorly, each specimen was left to cool down in air to room temperature and subjected to tensile testing up to failure. From these tests, mechanical parameters and stress-strain curves were obtained.

Post-fire tests were conducted at $\sigma_t = 0$ (PFU) and $\sigma_t \neq 0$ (PFL). From the results obtained in this work, the following conclusions can be drawn.

First of all, it is emphasized that different production routes of steels lead to different critical temperatures θ_{crit}, and also post-fire behaviours. Each steel type should be particularly tested, and the respective equations that characterize the behaviour of the material at high temperatures should be provided in the structural codes.

When heated to high temperatures, specimens regain a considerable amount of its initial mechanical properties after cooling down from target temperatures θ_t up to 700 °C. This is particularly evident for the case of modulus of elasticity E. Nevertheless, this is observed in PFU tests, whose conditions do not reflect realistic situations of steel structures during fire.

In PFL tests, it is seen that a reduction of the degree of utilisation μ_0 plays a favourable effect in the post-fire behaviour of the tested steels. This is, the lower is the load carried out by a structural element at the onset of fire, the higher is the recovery of the material after fire. Thus, for a structural member that carries out certain amount of load, a reduction of the degree of utilisation can be achieved by oversizing the section.

A special attention is put on the residual ductility of the steel after it was subjected to a combination of high temperature and tensile stress. PFL test results have shown that residual ductility of steel in a post-fire scenario can drop to values below the minimum required by the current standards. This can occur even in low-to-moderate intensity fires – maximum temperatures reached of 500 °C – in combination with a degree of utilisation not excessively elevated ($\mu_0 = 0.5$). The aforementioned aspects should be considered in the design of structures located in seismic hazard areas, for which ductility is a key feature.

References

[1] Smith, C. I.; Kirby, B. R.; Lapwood, D. G.; Cole, K. J.; Cunningham, A. P. and Preston. R. R. (1981) *The reinstatement of fire damaged steel framed structures.* Fire Safety Journal **4**. 21-62.

[2] Gosain, N. K.; Drexler, R. F. and Choudhuri, D. (2008) *Evaluation and Repair of Fire-Damaged Buildings.* Structure. 18-22.

[3] Tide, RHR. (1998) *Integrity of structural steel after exposure to fire.* Engineering Journal. 26-38.

[4] British Standard Institution (2003) *BS 5950-8. Structural use of steelwork in building: code of practice for fire resistant design.*

[5] Dill, F. H. (1960) *Structural steel after a fire.* In: Proceedings of AISC national engineering conference. 78-80.

[6] Gunalan, S. and Mahendran, M. (2014) *Experimental investigation of post-fire mechanical properties of cold-formed steels.* Thin-Walled Structures **84**. 241-254.

[7] Ren, C.; Dai, L.; Huang, Y. and He, W. (2020) *Experimental investigation of post-fire mechanical properties of Q235 cold-formed steel.* Thin-Walled Structures **150**. 1066551.

[8] Outinen, J. and Makelainen, P. (2004) *Mechanical properties of structural steel at elevated temperatures and after cooling down.* Fire and Materials **28**. 237-251.

[9] Tao, Z.; Wang, X. Q. and Uy, B. (2013) *Stress-strain curves of structural and reinforcing steels after exposure to elevated temperatures.* Journal of Materials in Civil Engineering **25**. 1306-1316.

[10] Maraveas, C.; Fasoulakis, Z. and Tsavdaridis. K. D. (2017) *Post-fire assessment and reinstatement of steel structures.* Journal of Structural Fire Engineering **8**. 181-201.

[11] Chiew, S. P.; Zhao, M. S. and Lee, C. K. (2014) *Mechanical properties of heat-treated high strength steel under fire/post-fire conditions.* Journal of Constructional Steel Research **98**. 12-19.

[12] Zhang, C.; Wang, R. and Song, G. (2020) *Post-fire mechanical properties of Q460 and Q690 high strength steels after fire-fighting foam cooling.* Thin-Walled Structures **156**. 106983.

[13] Wang, X.-Q.; Tao, Z.; Song, T.-Y. and Han, L.-H. (2014) *Stress-strain model of austenitic stainless steel after exposure to elevated temperatures.* Journal of Constructional Steel Research **99**. 129-139.

[14] European Comittee for Standardization (2005) *EN 1993-1-1. Eurocode 3: design of steel structures. Part 1-1: general rules – rules for buildings.*

[15] Lapuebla-Ferri, A.; Pons, D. and Romero, M. L. (2021) *Load and temperature influence on the post-fire mechanical properties of steel reinforcements.* Journal of Constructional Steel Research **185**. 106866.

[16] European Comittee for Standardization (2005) *EN 1993-1-2. Eurocode 3: design of steel structures. Part 1-2: general rules – structural fire design.*